

Technical Report on Visual Quality Assessment for Frame Interpolation

Hui Men¹, Hanhe Lin¹, Vlad Hosu¹, Daniel Maurer², Andrés Bruhn², Dietmar Saupe¹

¹Department of Computer and Information Science, University of Konstanz, Germany

²Institute for Visualization and Interactive Systems, University of Stuttgart, Germany

Email: {hui.3.men, hanhe.lin, dietmar.saupe}@uni-konstanz.de, {Andres.Bruhn, maurerdl}@vis.uni-stuttgart.de

Abstract—Current benchmarks for optical flow algorithms evaluate the estimation quality by comparing their predicted flow field with the ground truth, and additionally may compare interpolated frames, based on these predictions, with the correct frames from the actual image sequences. For the latter comparisons, objective measures such as mean square errors are applied. However, for applications like image interpolation, the expected user’s quality of experience cannot be fully deduced from such simple quality measures. Therefore, we conducted a subjective quality assessment study by crowdsourcing for the interpolated images provided in one of the optical flow benchmarks, the Middlebury benchmark. We used paired comparisons with forced choice and reconstructed absolute quality scale values according to Thurstone’s model using the classical least squares method. The results give rise to a re-ranking of 141 participating algorithms w.r.t. visual quality of interpolated frames mostly based on optical flow estimation. Our re-ranking result shows the necessity of visual quality assessment as another evaluation metric for optical flow and frame interpolation benchmarks.

Index Terms—visual quality assessment, optical flow, frame interpolation

I. INTRODUCTION

As one of the basic video processing techniques, frame interpolation, namely computing interpolated in-between images, is a necessary step in numerous applications such as temporal up-sampling for generating slow motion videos, frame rate conversion between broadcast standards and so on [1]. One of the main approaches in frame interpolation is motion compensation, which can be achieved in various ways based on block matching, frequency domain, optical flow, etc. [2] Among them, optical flow is the most popular one for this usage [1]. Typically, optical flow or its variations are estimated and then used to produce interpolation results. Thus, for a given frame interpolation technique, the quality of the results heavily depends on the optical flow algorithm adopted [3].

Regarding the evaluation of motion-compensated interpolation, currently, there is only one optical flow benchmark that is commonly used and offers an assessment of interpolated frames, which is the Middlebury benchmark [4]. It considers angular and endpoint errors between an estimated flow vector and the ground-truth flow to assess the accuracy of optical flow computation methods.

Moreover, it uses the estimated flow field to interpolate an in-between image for two video frames, and then computes the root mean square error (RMSE) and gradient normalized

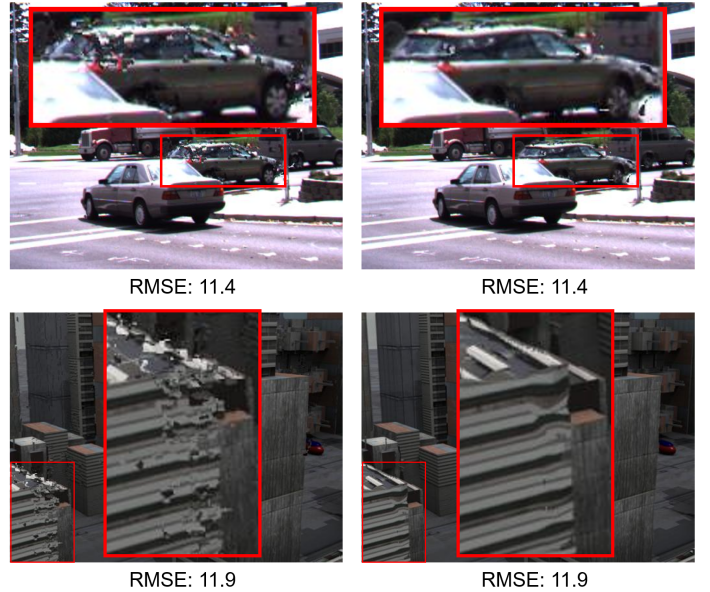


Fig. 1. Two interpolated frames, each with two different methods. RMSE values in each pair are equal, but the visual quality differs in each pair, in particular in the zoomed regions.

RMSE between the interpolated image and the ground-truth image. However, it is well known that mean square errors can be misleading and may not reliably reflect image quality as perceived by the human visual system (HVS) [5]. In the Middlebury interpolation evaluation web-page, some interpolated images have the same RMSE, but exhibit obvious differences in image quality (see Fig.1). Therefore, we propose that the evaluation of motion-compensated interpolation should take perceived visual quality assessment into consideration.

Regarding visual quality assessment methods, we take full-reference image quality assessment (FR-IQA) into consideration, since ground-truth in-between images are available in the Middlebury benchmark. There are several FR-IQA methods that consider the HVS, such as SSIM [5], MS-SSIM [6], FSIM [7], VSI [8]. These methods were designed to estimate image quality degradation due to common artifacts, namely the ones caused by processing such as data compression or by losses in data transmission. However, the artifacts induced by optical flow algorithms lead to interpolated images with different specific distortions.

TABLE I
SROCC BETWEEN FR-IQA AND GROUD-TRUTH (BY SUBJECTIVE STUDY)

FR-IQA	Average	Mequon	Schefflera	Urban	Teddy	Backyard	Basketball	Dumptruck	Evergreen
RMSE	0.598	0.766	0.557	0.854	0.667	0.152	0.534	0.756	0.494
SSIM	0.592	0.747	0.552	0.718	0.566	0.255	0.693	0.788	0.416
MS-SSIM	0.602	0.733	0.491	0.741	0.653	0.260	0.698	0.795	0.444
FSIM	0.599	0.739	0.573	0.783	0.631	0.244	0.553	0.778	0.488
VSI	0.610	0.705	0.558	0.803	0.657	0.204	0.615	0.783	0.555

In this contribution, we show (in Table I) that five objective FR-IQA methods have rather low correlations with the evaluations made by human observers, regardless of whether the methods are based on the HVS or just on pixel-wise errors such as RMSE. More specifically, the method VSI, one of the best FR-IQA methods, when trained and tested on the LIVE database [9], yielded a Spearman rank-order correlation coefficient (SROCC) of 0.952 w.r.t. ground truth consisting of MOS from a controlled lab study for the LIVE database. But when applied for the interpolated images by optical flow algorithms, VSI gave only an SROCC of 0.610. This shows that current FR-IQA methods do not perform well on interpolated frames produced by optical flow algorithms because of their specific distortions. Therefore, a new FR-IQA method specifically designed for such images is needed. However, before the research in such FR-IQA methods can proceed, ground-truth data, namely subjective quality scores of such images need to be collected, a first set of which is provided by our study.

For subjective quality evaluation, lab-studies take the lead because of their reliability. In lab-studies, the experimental environment and the evaluation process can be controlled. However, it is time consuming and costly, which severely limits the number of images to be assessed. Crowdsourcing studies can be less expensive and the reliability of crowdsourcing has been proven to be acceptable with appropriate setup and certain training for the crowd workers [10]. Therefore, we applied subjective quality assessment of the images interpolated by optical flow algorithms with the help of crowdsourcing.

In this paper, we implemented paired comparisons of the interpolated images given by optical flow algorithms in the Middlebury interpolation benchmark with the help of crowdsourcing and re-ranked them accordingly. After that, the old ranking according to RMSE in the Middlebury benchmark and the re-ranking according to our subjective study were compared. After that, the old ranking according to RMSE in the Middlebury benchmark and the re-ranking according to our subjective study were compared. Our study shows that current FR-IQA methods are not suitable for assessing the perceived visual quality of interpolated frames (as produced by optical flow algorithms).

II. RELATED WORK

So far, there is only one benchmark that is used for evaluating the performance of frame interpolation, namely the Middlebury benchmark. It was originally designed for the evaluation of optical flow algorithms. Since it provides the

ground-truth in-between images to evaluate the interpolation performance of optical flow algorithms, some interpolation algorithms also made use of this benchmark for evaluation, [11], [1], [3].

Some interpolation algorithms like [12], [13] used the UCF 101 dataset [14] for training and testing. Others like [11], [15], [16] used the videos from [17], [18]. For evaluation, generally they chose to compute one of MSE, PSNR, and SSIM between their interpolated images and the ground-truth in-between images.

III. SUBJECTIVE STUDY USING PAIRED COMPARISONS

A. Subjective Study

Absolute Category Rating (ACR) is a judgment where the test items are presented one at a time and are rated independently on a category of five ordinal scales, i.e., Bad-1, Poor-2, Fair-3, Good-4, and Excellent-5 [19].

ACR is easy and fast for implementation, however, it has several problems [20]. Participants may be confused when the concept of the ACR scale has not been explained sufficiently well. They may also have different interpretations of the ACR scale, in particular in crowdsourcing experiments because of the wide range of backgrounds and perceptual experiences of the crowd workers from around the world. Moreover, the perceptual distances between two consecutive scale values, e.g., between 1 and 2, should ideally be the same. However, in practice this can hardly be achieved [21]. Also it is not easy to detect when a participant intentionally or carelessly gives false ratings.

Alternatively, *paired comparisons* (PC) can solve some of the problems of ACR. In a PC test, items to be evaluated are presented as pairs. In a forced choice setting, one of the items must be chosen as the preferred one. The main advantage of this is that it is highly discriminatory, which is very relevant when test items have nearly the same quality.

However, when implemented naively, to compare N items would require $\binom{N}{2}$ comparisons, too many to be practical, when N is on the order of 100, for example. In our case, for each of the 8 sequences, we would have to compare $N = 141$ images, giving a total of 78,960 pairs.

Instead, random paired comparisons randomly chooses a fraction of all possible paired comparisons. This is more efficient and has been proven to be as reliable as full comparisons [22]. After obtaining paired comparisons results, subjective quality scores can be reconstructed based on Thurstone's model [23], [24] or the Bradley-Terry model [25].

B. Thurstone's Model

Thurstone's model provides the basis for a psychometric method for assigning scale values to options on a one-dimensional continuum from paired comparisons data. It assumes that an option's quality is a Gaussian random variable, thereby accommodating differing opinions about the quality of an option. Then each option's latent quality score is revealed by the mean of the corresponding Gaussian.

The result of a paired comparison experiment is a square count matrix C denoting the number of times that each option was preferred over any other option. More specifically, for n comparisons of option A_i with option A_j , $C_{i,j}$ gives the number of times A_i was preferred over A_j . Similarly, $C_{j,i}$ in the count matrix denotes the number of times that A_j was preferred over A_i , and we have $C_{i,j} + C_{j,i} = n$.

According to Thurstone' Case V, subjective qualities about two options A and B are modelled as uncorrelated Gaussian random variables A and B with mean opinions μ_A, μ_B and variances σ_A^2, σ_B^2 , respectively. When individuals decide which of the two options is better, they draw realizations from their quality distributions, and then choose the option with higher quality. More specifically, they choose option A over option B if their draw from the random variable $A - B$ (with mean $\mu_{AB} = \mu_A - \mu_B$ and variance $\sigma_{AB}^2 = \sigma_A^2 + \sigma_B^2$) is greater than 0. Therefore, the probability of a subject to prefer option A over B is:

$$P(A > B) = P(AB > 0) = \Phi\left(\frac{\mu_{AB}}{\sigma_{AB}}\right), \quad (1)$$

where $\Phi(\cdot)$ is the standard normal cumulative distribution function (CDF).

Thurstone proposed to estimate $P(A > B)$ by the empirical proportion of people preferring A over B, which can be derived from the count matrix C as

$$P(A > B) \approx \frac{C_{A,B}}{C_{A,B} + C_{B,A}}.$$

The estimated quality difference $\hat{\mu}_{AB}$ can be derived from inverting Eq. 1, giving:

$$\hat{\mu}_{AB} = \sigma_{AB}\Phi^{-1}\left(\frac{C_{A,B}}{C_{A,B} + C_{B,A}}\right)$$

known as Thurstones Law of Comparative Judgment, where $\Phi(\cdot)^{-1}$ is the inverse standard normal CDF, or z-score. Least-squares fitting or maximum likelihood estimation (MLE) can be then applied to estimate the scale values μ_A for all involved stimuli A . For more details we refer to the technical report [26].

C. Study Design

In order to re-rank the methods in the Middlebury benchmark, we implemented paired comparisons based on Thurstone's model with least-squares estimation to obtain subjective judgments of the image qualities. In the benchmark, there are 8 sets of interpolated images, most of which generated by



Which of the two images has a better quality? (required)

- the left
- the right

Fig. 2. Crowdsourcing interface.

Compare Pairs Of Images
Instructions
Overview
We need your help to compare pairs of images. Try to quickly answer the question. We are interested in your first impression.
Specifically, you can pay more attention to the part in the red circle:

Fig. 3. Instructions of the crowdsourcing experiment.

141 optical flow methods.¹ Therefore, in our experiment, for each set of 141 interpolated images, we generated a random sparse graph with degree of 6 (i.e., each image was to be randomly compared to 6 other images), which resulted in 423 pairs of images. We ran the experiment using the Figure Eight [27] platform. In our crowdsourcing interface as shown in Fig. 2, crowd workers were asked to identify and select the image with better quality for each image pair (forced binary choice).

D. Quality Assurance and Quality Control

Before the actual paired comparison, there was a training session, in which workers were instructed how to compare the image quality. Since the visual differences between some images are not that obvious, in the instructions as shown in Fig. 3, we highlighted those parts in the images that are more degraded and hence showed more differences.

In our experiment, we had eight separate jobs, each containing the 423 image pairs of the same series. In each job, there were 22 tasks, each consists of one page. In order to make sure that crowd workers' performance was not effected by exhaustion, we showed 20 pairs of images per page, and payments were initiated for each completed page. For each pair of images to be compared, we collected 30 votes from the crowd workers.

¹Note that when we ran the experiments in June 2018, there were altogether 141 methods in the Middlebury benchmark, which now includes a number of additional, new methods.

In order to assure the reliability of the crowd workers, the unreliable ones need to be detected and disallowed to continue. This was done by requiring crowd workers to answer test questions. For the test questions we chose image pairs with the ground-truth in-between image as one of the images, and the other image of bad quality. Then the expected, correct answer was obviously given by choosing the ground-truth image as the one with a better quality.

Before crowd workers were allowed to start a job, they must pass a quiz which is composed entirely of test questions. This ensures that only crowd workers that proved to be able to work on the subject matter of the job, would be able to enter the job. Crowd workers that failed the quiz were permanently disqualified from working on the job. After passing the quiz, crowd workers were admitted to start the real job. During the job, they had to answer further hidden test questions. Once a crowd worker failed more than 30% of the hidden test questions, he or she was disqualified and removed from the job. Only crowd workers who passed the quiz and showed an accuracy above 70% on the hidden test questions were regarded as reliable.

IV. RESULTS

A. Statistics for the Crowdsourcing Experiment

In our experiment, there were eight jobs, each one comparing 141 interpolated images pairwise (423 pairs per job). The average run time was 29 hours per job. In total, 3189 crowd workers participated in our experiment, some of them took multiple jobs. Before the real experiment, 54% of them did not pass the quiz thus were not allowed to contribute to the job. During the real job, 14% of them failed more than 30% of the test questions, thus been disregarded. In the end, 1033 crowd workers were accepted as trusted workers. Among the trusted workers, 79% had an accuracy of 90%-100% (where 100% means they passed all test questions), 10% of them had an accuracy of 80%-90% and 10% of them had an accuracy of 70%-80%.

B. Re-ranking Results

Given the results of the paired comparisons, we reconstructed corresponding quality values based on Thurstone's model using the code provided by [26]. In order to make the results of the 8 separate jobs comparable, we added two fictitious images as anchors. One of them represents the worst quality among all the images, and the other one is like the ground-truth image, with a quality that is better than that of all the other images. After reconstruction of the scale values for the 141 + 2 images in each series, we linearly rescaled the quality scores such that the quality of the imaginary worst quality image became 0, and that of the ground-truth image became 1. In this way, we rescaled the reconstructed scores to the interval [0, 1]. Reconstructed quality values are shown in Table IV and V, accompanied by their corresponding rankings. Note that for each set, we ranked them separately. The 'Average' in the first column was gained by taking the

mean of the 8 quality values in the same row, which results in the rank according to average quality.

Table VI and VII show the differences between the re-ranking (ranked according to subjective study) and their corresponding ranking in the Middlebury benchmark (ranked according to RMSE), denoted by 'new' and 'old' in the tables, respectively. It can be seen that the best three methods ranked by the subjective study (i.e., SuperSlomo, CtxSyn and DeepFlow2), ranked 1st, 5th and 9th in the Middlebury benchmark, respectively. Overall, 36 methods highlighted in color blue showed rank differences up to 5. However, 30 methods highlighted in color red gave differences of more than 30 between their new and old rankings.

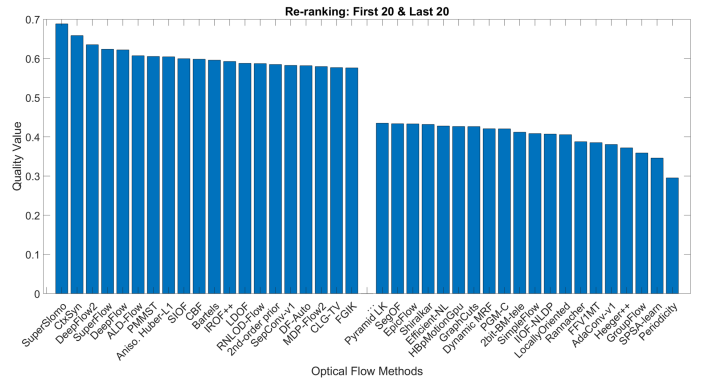


Fig. 4. The methods ranking in the top 20 and the bottom 20 by the subjective study. The x-axis shows the names of the methods. The y-axis denotes the value of the average subjective scores.

Fig. 4 shows the subjective qualities of the methods ranked the highest 20 and the lowest 20. The quality scores of the best two methods, SuperSlomo and CtxSyn, are better than those of the rest by a large margin.

As an overall analysis, Table II shows the bootstrapped (after 1000 iterations) SROCC correlation values accompanied with confidence intervals (95%) between the ranking in Middlebury benchmark (i.e., ranking according to RMSE) and the re-ranking according to our subjective study. Note that the confidence interval of SROCC was computed by transforming the rank correlation score into an approximate z-score using the Fisher transform [28]. In a nutshell, a confidence interval of probability p is given by $\tanh(\arctan r \pm \Phi^{-1}(p)/\sqrt{n-3})$, where r denotes the estimated SROCC, n is the sampling size, and Φ^{-1} is the inverse of the standard normal CDF. In order to visualize the result, we computed the disagreement level as $1 - SROCC$ as shown in Fig. 5.

Fig. 6 shows the scatter plots of the RMSE values compared to subjective scores of each optical flow method. Those eight plots are displayed in descending order of SROCC between RMSE and subjective scores. It can be seen that starting from *Urban* with the highest SROCC (0.854) down to the lowest SROCC (0.152) given by *Backyard*, the scattered plots become more sparse, as to be expected from their decreasing correlation.

TABLE II
BOOTSTRAPPED CORRELATIONS BETWEEN RMSE AND GROUND-TRUTH (BY SUBJECTIVE STUDY) AFTER 1000 ITERATIONS

RMSE	Average	Mequon	Schefflera	Urban	Teddy	Backyard	Basketball	Dumptruck	Evergreen
SROCC	0.598	0.766	0.557	0.854	0.667	0.152	0.534	0.756	0.494
CI 95%	[0.507,0.674]	[0.699,0.816]	[0.454,0.647]	[0.813,0.888]	[0.581,0.737]	[0.015,0.283]	[0.419,0.618]	[0.695,0.813]	[0.382,0.593]

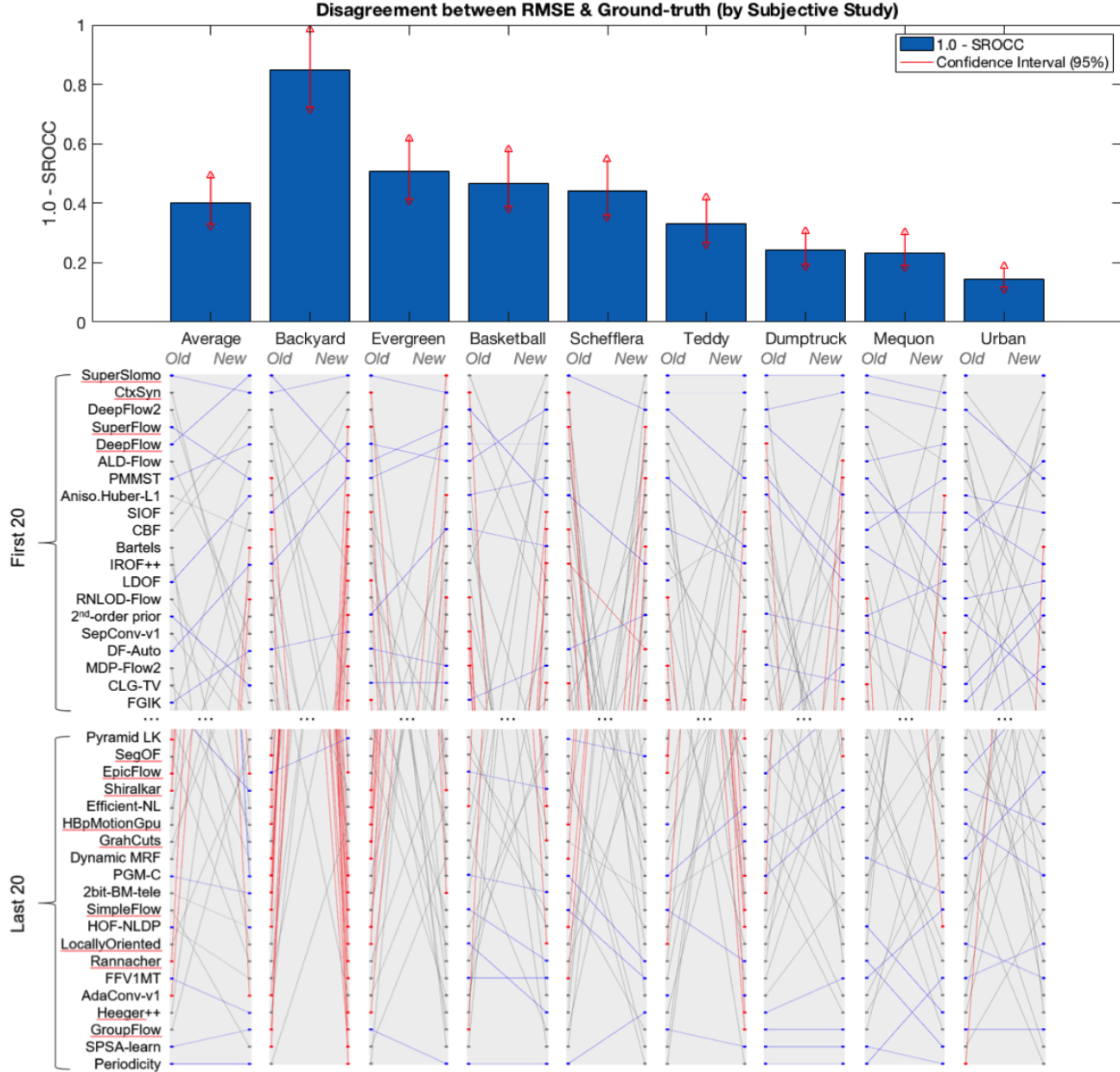


Fig. 5. Disagreement level and corresponding ranking differences. Upper bars: disagreement level with 95% confidence interval. Lower graphs: nodes on the left side denote their old ranking in the Middlebury benchmark Nodes on the right side denote their new ranking by subjective study. Lines in blue color denote the ranking differences are less than 5, and lines in color red denote the ranking differences are larger than 50.

TABLE III
RESOLUTIONS OF THE ORIGINAL IMAGES AND THE AVAILABLE ONES USED FOR SUBJECTIVE STUDY

	Mequon	Schefflera	Urban	Teddy	Backyard	Basketball	Dumptruck	Evergreen
Original	584×388	584×388	640×480	420×360	640×480	640×480	640×480	640×480
Available	467×310	467×310	512×384	336×288	512×384	512×384	512×384	512×384

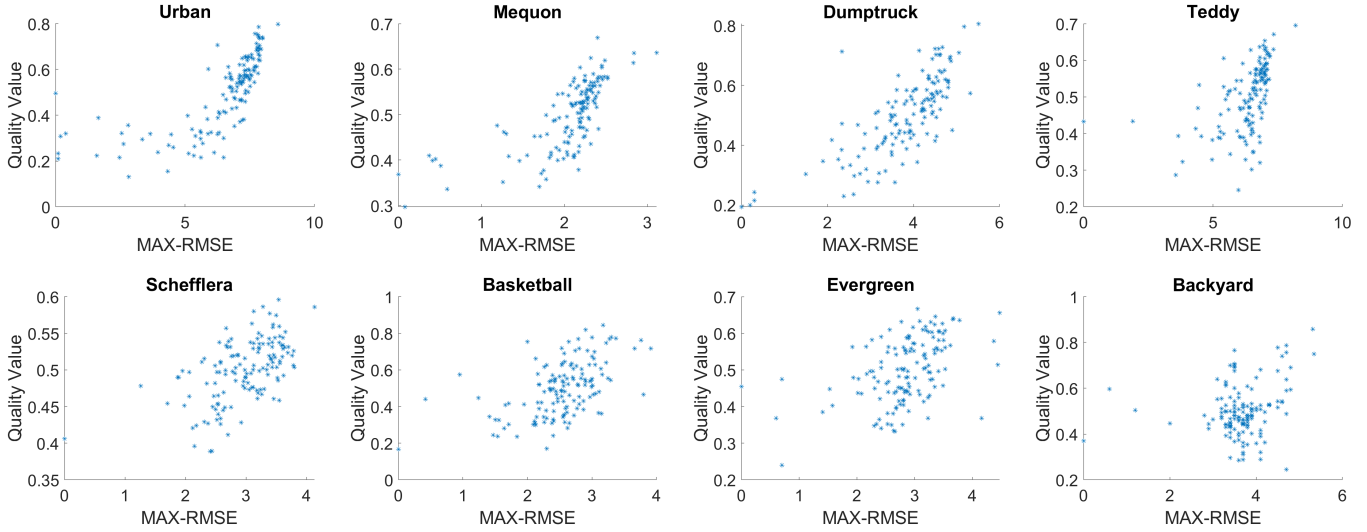


Fig. 6. Scatter plots of RMSE and subjective scores. To show positive correlations, we used the difference between maximum and individual RMSE as the x-axis values.

V. LIMITATIONS

The interpolated images available from the Middlebury benchmark are compressed and slightly downsized from the original images. The original interpolated images could not be made available by the maintainers of the Middlebury benchmark. The differences between their resolutions are shown in Table III. Since we used the downscaled, compressed public version of the images for the crowdsourcing study, our results may be biased to a small extent.

Another limitation of the experiment is the difficulty of the subjective study. The quality differences between some images are quite hard to distinguish. Therefore, in the instructions of the crowdsourcing experiment, we highlighted the main degraded parts according to our visual observation to help the crowd workers to focus on the critical parts of the images. We believe, that this can be further improved in future studies, e.g., by providing zoomed image portions that contain the most noticeable artifacts.

VI. CONCLUSION AND FUTURE WORK

We have adopted visual quality assessment to the Middlebury benchmark for frame interpolation based mostly on optical flow methods. Our study confirms that only using RMSE as an evaluation metric for image interpolation performance is not representative of visual quality. Also current FR-IQA methods do not provide satisfying results on those interpolated images. This is due to the fact that such images, especially the ones generated by optical flow algorithms have specific distortions that are quite different from artifacts commonly addressed by conventional IQA methods.

Therefore, we plan to develop a domain specific FR-IQA for frame interpolation based on optical flow estimation. For the reference there is the original ground truth frame. In addition, we can make use of the ground truth optical flow vector field which is also available for the frame to be interpolated.

This amounts to a FR-IQA with side information given by optical flow. It requires feature extraction from images and additionally from the optical flow, in order to train a model for a FR-IQA method specifically for frame interpolation by means of optical flow. The use case of such a FR-IQA method is to serve as a visual quality metric in optical flow benchmarks. Moreover, we plan to apply VQA methods on the videos generated by frame interpolation as a further study. This, in turn, will allow us to consider temporal aspects in the quality assessment.

ACKNOWLEDGMENT

Funded by the Deutsche Forschungsgemeinschaft (DFG, German Research Foundation) – Projektnummer 251654672 – TRR 161 (Project A05 and B04).

REFERENCES

- [1] S. Meyer, O. Wang, H. Zimmer, M. Grosse, and A. Sorkine-Hornung, “Phase-based frame interpolation for video,” in *Proceedings of the IEEE Conference on Computer Vision and Pattern Recognition*, 2015, pp. 1410–1418.
- [2] F. Dufaux and F. Moscheni, “Motion estimation techniques for digital TV: A review and a new contribution,” *Proceedings of the IEEE*, vol. 83, no. 6, pp. 858–876, 1995.
- [3] S. Niklaus and F. Liu, “Context-aware synthesis for video frame interpolation,” in *Proceedings of the IEEE Conference on Computer Vision and Pattern Recognition (CVPR)*, 2018, pp. 1701–1710.
- [4] S. Baker, D. Scharstein, J. Lewis, S. Roth, M. J. Black, and R. Szeliski, “A database and evaluation methodology for optical flow,” *International Journal of Computer Vision*, vol. 92, no. 1, pp. 1–31, 2011.
- [5] Z. Wang, A. C. Bovik, H. R. Sheikh, and E. P. Simoncelli, “Image quality assessment: from error visibility to structural similarity,” *IEEE Transactions on Image Processing*, vol. 13, no. 4, pp. 600–612, 2004.
- [6] Z. Wang, E. P. Simoncelli, and A. C. Bovik, “Multiscale structural similarity for image quality assessment,” in *Proceeding of the IEEE Asilomar Conference on Signals (ACSSC), Systems & Computers*, 2003, pp. 1398–1402.
- [7] L. Zhang, L. Zhang, X. Mou, and D. Zhang, “FSIM: a feature similarity index for image quality assessment,” *IEEE Transactions on Image Processing*, vol. 20, no. 8, pp. 2378–2386, 2011.

- [8] L. Zhang, Y. Shen, and H. Li, "VSI: A visual saliency-induced index for perceptual image quality assessment," *IEEE Transactions on Image Processing*, vol. 23, no. 10, pp. 4270–4281, 2014.
- [9] H. R. Sheikh, M. F. Sabir, and A. C. Bovik, "A statistical evaluation of recent full reference image quality assessment algorithms," *IEEE Transactions on Image Processing*, vol. 15, no. 11, pp. 3440–3451, 2006.
- [10] D. Saupe, F. Hahn, V. Hosu, I. Zingman, M. Rana, and S. Li, "Crowd workers proven useful: A comparative study of subjective video quality assessment," in *the 8th International Conference on Quality of Multimedia Experience (QoMEX)*, 2016.
- [11] L. L. Rakêt, L. Roholm, A. Bruhn, and J. Weickert, "Motion compensated frame interpolation with a symmetric optical flow constraint," in *International Symposium on Visual Computing*. Springer, 2012, pp. 447–457.
- [12] Z. Liu, R. A. Yeh, X. Tang, Y. Liu, and A. Agarwala, "Video frame synthesis using deep voxel flow," in *Proceedings of the IEEE International Conference on Computer Vision (ICCV)*, 2017, pp. 4463–4471.
- [13] Z. Gong and Z. Yang, "Video frame interpolation and extrapolation," Stanford University, Tech. Rep., 2017. [Online]. Available: <http://cs231n.stanford.edu/reports/2017/pdfs/714.pdf>
- [14] K. Soomro, A. R. Zamir, and M. Shah, "UCF101: A dataset of 101 human actions classes from videos in the wild," *arXiv preprint arXiv:1212.0402*, 2012.
- [15] J. Zhai, K. Yu, J. Li, and S. Li, "A low complexity motion compensated frame interpolation method," in *Proceedings of the IEEE International Symposium on Circuits and Systems (ISCAS)*, 2005, pp. 4927–4930.
- [16] R. C. Ghutke, C. Naveen, and V. R. Satpute, "A novel approach for video frame interpolation using cubic motion compensation technique," *International Journal of Applied Engineering Research*, vol. 11, no. 10, pp. 7139–7146, 2016.
- [17] <http://see.xidian.edu.cn/vipsl/dataset.html>.
- [18] http://see.xidian.edu.cn/vipsl/database_Video.html.
- [19] P. ITU-T RECOMMENDATION, "Subjective video quality assessment methods for multimedia applications," Tech. Rep., 1999. [Online]. Available: <https://www.itu.int/rec/T-REC-P.910-200804-I>
- [20] K.-T. Chen, C.-C. Wu, Y.-C. Chang, and C.-L. Lei, "A crowdsourceable QoE evaluation framework for multimedia content," in *Proceedings of the ACM International Conference on Multimedia (MM)*, 2009, pp. 491–500.
- [21] T. Hoßfeld, P. E. Heegaard, M. Varela, and S. Möller, "QoE beyond the MOS: an in-depth look at QoE via better metrics and their relation to MOS," *Quality and User Experience*, vol. 1, no. 2, pp. 1–23, 2016.
- [22] Q. Xu, Q. Huang, T. Jiang, B. Yan, W. Lin, and Y. Yao, "Hodgerank on random graphs for subjective video quality assessment," *IEEE Transactions on Multimedia*, vol. 14, no. 3, pp. 844–857, 2012.
- [23] L. L. Thurstone, "A law of comparative judgment." *Psychological Review*, vol. 34, no. 4, p. 273, 1927.
- [24] R. D. Luce, "Thurstone and sensory scaling: Then and now." *US: American Psychological Association*, vol. 101(2), pp. 271–277, 1994.
- [25] R. A. Bradley and M. E. Terry, "Rank analysis of incomplete block designs: I. the method of paired comparisons," *Biometrika*, vol. 39, no. 3/4, pp. 324–345, 1952.
- [26] K. Tsukida and M. R. Gupta, "How to analyze paired comparison data," University of Washington, Tech. Rep., 2011. [Online]. Available: <https://www.itu.int/rec/T-REC-P.910-200804-I>
- [27] <https://www.figure-eight.com/>.
- [28] J. Ruscio, "Constructing confidence intervals for spearman's rank correlation with ordinal data: a simulation study comparing analytic and bootstrap methods," *Journal of Modern Applied Statistical Methods*, vol. 7, no. 2, p. 7, 2008.

TABLE IV
SUBJECTIVE QUALITY VALUES AND THE RE-RANKING OF THE MIDDLEBURY BENCHMARK (PART I).

	Average value / rank	Mequon value / rank	Schefflera value / rank	Urban value / rank	Teddy value / rank	Backyard value / rank	Basketball value / rank	Dumptruck value / rank	Evergreen value / rank
SuperSlomo	0.688 / 1	0.635 / 3	0.504 / 71	0.798 / 1	0.671 / 2	0.750 / 6	0.763 / 8	0.806 / 1	0.579 / 32
CtxSyn	0.658 / 2	0.636 / 2	0.586 / 3	0.464 / 91	0.695 / 1	0.858 / 1	0.718 / 13	0.796 / 2	0.515 / 61
DeepFlow2	0.635 / 3	0.571 / 26	0.530 / 39	0.736 / 9	0.590 / 23	0.596 / 26	0.780 / 3	0.648 / 18	0.631 / 9
SuperFlow	0.624 / 4	0.583 / 13	0.476 / 104	0.501 / 82	0.554 / 46	0.756 / 5	0.777 / 4	0.703 / 10	0.638 / 5
DeepFlow	0.622 / 5	0.535 / 51	0.550 / 13	0.692 / 16	0.605 / 17	0.532 / 38	0.747 / 11	0.709 / 8	0.603 / 21
ALD-Flow	0.607 / 6	0.565 / 27	0.586 / 2	0.660 / 22	0.609 / 15	0.417 / 116	0.845 / 1	0.696 / 12	0.479 / 82
PMMST	0.605 / 7	0.608 / 7	0.534 / 31	0.690 / 17	0.504 / 77	0.638 / 19	0.772 / 5	0.593 / 32	0.502 / 68
Aniso. Huber-L1	0.604 / 8	0.579 / 18	0.534 / 32	0.614 / 35	0.617 / 12	0.521 / 47	0.641 / 24	0.702 / 11	0.626 / 10
SIOF	0.599 / 9	0.538 / 49	0.531 / 36	0.657 / 24	0.586 / 25	0.690 / 12	0.662 / 21	0.563 / 45	0.568 / 35
CBF	0.598 / 10	0.580 / 17	0.529 / 40	0.705 / 12	0.610 / 14	0.593 / 27	0.575 / 40	0.611 / 29	0.582 / 30
Bartels	0.596 / 11	0.486 / 86	0.538 / 22	0.683 / 18	0.524 / 64	0.740 / 7	0.495 / 73	0.727 / 3	0.573 / 33
IROF++	0.592 / 12	0.625 / 4	0.575 / 6	0.541 / 71	0.630 / 7	0.477 / 77	0.769 / 6	0.644 / 19	0.478 / 83
LDOF	0.588 / 13	0.571 / 25	0.482 / 98	0.468 / 89	0.640 / 4	0.787 / 2	0.706 / 17	0.484 / 80	0.561 / 41
RNLOD-Flow	0.587 / 14	0.493 / 80	0.580 / 4	0.621 / 33	0.575 / 33	0.700 / 10	0.547 / 52	0.622 / 24	0.558 / 44
2nd-order prior	0.585 / 15	0.583 / 14	0.503 / 72	0.609 / 38	0.536 / 60	0.609 / 23	0.508 / 70	0.722 / 5	0.608 / 16
SepConv-v1	0.582 / 16	0.614 / 6	0.486 / 95	0.496 / 83	0.629 / 8	0.488 / 68	0.717 / 15	0.574 / 41	0.656 / 2
DF-Auto	0.582 / 17	0.469 / 95	0.563 / 7	0.598 / 41	0.542 / 55	0.778 / 3	0.629 / 28	0.494 / 78	0.581 / 31
MDP-Flow2	0.579 / 18	0.577 / 19	0.492 / 89	0.668 / 20	0.614 / 13	0.590 / 28	0.551 / 49	0.689 / 13	0.454 / 95
CLG-TV	0.577 / 19	0.549 / 41	0.485 / 96	0.583 / 47	0.635 / 6	0.480 / 74	0.554 / 46	0.703 / 9	0.624 / 11
FGIK	0.576 / 20	0.583 / 15	0.465 / 113	0.324 / 112	0.606 / 16	0.676 / 15	0.719 / 12	0.713 / 7	0.521 / 59
IROF-TV	0.572 / 21	0.532 / 53	0.519 / 50	0.693 / 15	0.618 / 11	0.509 / 54	0.622 / 32	0.532 / 61	0.553 / 49
LME	0.572 / 22	0.574 / 23	0.516 / 54	0.601 / 40	0.589 / 24	0.515 / 49	0.606 / 36	0.682 / 15	0.493 / 76
TC/T-Flow	0.572 / 23	0.526 / 59	0.543 / 19	0.754 / 4	0.494 / 79	0.452 / 94	0.820 / 2	0.425 / 103	0.559 / 43
Modified CLG	0.569 / 24	0.583 / 12	0.426 / 134	0.653 / 25	0.590 / 21	0.681 / 14	0.391 / 104	0.620 / 25	0.604 / 20
CombBMOF	0.563 / 25	0.484 / 87	0.560 / 9	0.560 / 61	0.598 / 18	0.496 / 65	0.706 / 16	0.555 / 50	0.545 / 54
CRTflow	0.562 / 26	0.549 / 40	0.531 / 34	0.509 / 79	0.518 / 68	0.467 / 82	0.699 / 18	0.633 / 20	0.590 / 25
p-harmonic	0.561 / 27	0.590 / 10	0.519 / 51	0.640 / 31	0.575 / 32	0.510 / 53	0.480 / 80	0.628 / 22	0.544 / 55
TV-L1-MCT	0.559 / 28	0.431 / 112	0.530 / 38	0.524 / 76	0.539 / 57	0.497 / 63	0.629 / 27	0.716 / 6	0.605 / 19
OAR-Flow	0.558 / 29	0.524 / 64	0.467 / 112	0.786 / 2	0.637 / 5	0.458 / 91	0.516 / 68	0.522 / 64	0.552 / 50
FMOF	0.557 / 30	0.604 / 8	0.534 / 30	0.352 / 108	0.575 / 29	0.542 / 35	0.754 / 9	0.572 / 42	0.520 / 60
NNF-Local	0.554 / 31	0.564 / 30	0.526 / 42	0.642 / 30	0.576 / 28	0.539 / 37	0.550 / 50	0.579 / 40	0.457 / 92
Brox et al.	0.553 / 32	0.515 / 71	0.546 / 14	0.573 / 51	0.590 / 22	0.526 / 41	0.487 / 75	0.546 / 56	0.641 / 4
DMF_ROB	0.548 / 33	0.545 / 45	0.506 / 66	0.706 / 11	0.518 / 67	0.481 / 73	0.471 / 81	0.580 / 39	0.572 / 34
TI-DOFE	0.547 / 34	0.422 / 114	0.490 / 91	0.579 / 48	0.528 / 62	0.526 / 42	0.636 / 25	0.587 / 33	0.610 / 14
WLIF-Flow	0.542 / 35	0.669 / 1	0.532 / 33	0.552 / 66	0.575 / 30	0.454 / 93	0.571 / 41	0.617 / 26	0.368 / 131
Ad-TV-NDC	0.542 / 36	0.412 / 118	0.516 / 56	0.746 / 5	0.565 / 39	0.290 / 138	0.518 / 66	0.722 / 4	0.567 / 36
MLDP_OF	0.541 / 37	0.537 / 50	0.495 / 85	0.695 / 13	0.509 / 73	0.559 / 31	0.536 / 59	0.561 / 47	0.434 / 111
TCOF	0.536 / 38	0.471 / 93	0.506 / 68	0.572 / 52	0.568 / 35	0.578 / 29	0.606 / 35	0.506 / 71	0.483 / 78
Local-TV-L1	0.536 / 39	0.530 / 54	0.494 / 87	0.736 / 8	0.653 / 3	0.318 / 135	0.452 / 88	0.494 / 77	0.607 / 17
Classic++	0.535 / 40	0.564 / 29	0.495 / 86	0.713 / 10	0.505 / 76	0.481 / 71	0.466 / 83	0.473 / 82	0.587 / 28
nLayers	0.529 / 41	0.554 / 37	0.529 / 41	0.602 / 39	0.560 / 43	0.612 / 22	0.444 / 90	0.520 / 65	0.414 / 119
2DHMM-SAS	0.529 / 42	0.574 / 21	0.489 / 93	0.372 / 106	0.565 / 38	0.509 / 55	0.717 / 14	0.550 / 53	0.454 / 94
Filter Flow	0.526 / 43	0.508 / 75	0.453 / 121	0.560 / 62	0.408 / 114	0.676 / 16	0.559 / 44	0.537 / 60	0.504 / 65
MDP-Flow	0.522 / 44	0.619 / 5	0.518 / 52	0.597 / 43	0.468 / 94	0.522 / 46	0.375 / 109	0.606 / 31	0.473 / 87
JOF	0.521 / 45	0.534 / 52	0.544 / 17	0.646 / 29	0.565 / 37	0.474 / 78	0.322 / 124	0.651 / 16	0.433 / 112
PH-Flow	0.521 / 46	0.450 / 107	0.531 / 35	0.695 / 14	0.549 / 48	0.516 / 48	0.379 / 108	0.624 / 23	0.424 / 114
TC-Flow	0.521 / 47	0.440 / 108	0.472 / 109	0.741 / 6	0.539 / 59	0.448 / 97	0.516 / 67	0.571 / 43	0.441 / 104
NN-field	0.521 / 48	0.563 / 32	0.506 / 67	0.428 / 95	0.472 / 89	0.543 / 34	0.548 / 51	0.609 / 30	0.496 / 74
Learning Flow	0.521 / 49	0.551 / 39	0.510 / 62	0.495 / 84	0.544 / 54	0.511 / 52	0.540 / 56	0.423 / 104	0.591 / 24
PGAM+LK	0.519 / 50	0.462 / 98	0.481 / 100	0.274 / 126	0.413 / 113	0.766 / 4	0.626 / 29	0.563 / 46	0.562 / 39
AGIF+OF	0.518 / 51	0.530 / 55	0.562 / 8	0.578 / 49	0.577 / 27	0.513 / 51	0.422 / 97	0.632 / 21	0.332 / 140
OFRF	0.517 / 52	0.408 / 123	0.497 / 82	0.478 / 86	0.488 / 83	0.553 / 33	0.754 / 10	0.513 / 69	0.450 / 99
BlockOverlap	0.517 / 53	0.525 / 62	0.539 / 21	0.544 / 69	0.545 / 53	0.482 / 70	0.351 / 114	0.512 / 70	0.636 / 6
NNF-EAC	0.513 / 54	0.561 / 33	0.460 / 117	0.460 / 92	0.457 / 97	0.362 / 130	0.769 / 7	0.560 / 48	0.475 / 85
TriFlow	0.512 / 55	0.452 / 105	0.498 / 80	0.659 / 23	0.389 / 125	0.458 / 92	0.543 / 55	0.514 / 68	0.588 / 27
ComplOF-FED-GPU	0.509 / 56	0.580 / 16	0.494 / 88	0.388 / 102	0.564 / 40	0.429 / 113	0.466 / 82	0.587 / 34	0.562 / 40
FlowFields+	0.505 / 57	0.525 / 60	0.459 / 118	0.562 / 60	0.471 / 90	0.465 / 85	0.533 / 61	0.585 / 35	0.440 / 105
Sparse-NonSparse	0.505 / 58	0.554 / 38	0.517 / 53	0.649 / 28	0.482 / 86	0.437 / 109	0.427 / 95	0.527 / 62	0.444 / 101
SILK	0.504 / 59	0.427 / 113	0.451 / 122	0.320 / 115	0.545 / 52	0.690 / 13	0.314 / 127	0.689 / 14	0.593 / 23
Occlusion-TV-L1	0.503 / 60	0.493 / 82	0.445 / 127	0.740 / 7	0.390 / 124	0.499 / 62	0.462 / 85	0.548 / 54	0.450 / 97
TF+OM	0.502 / 61	0.471 / 94	0.558 / 10	0.545 / 68	0.422 / 110	0.288 / 139	0.625 / 31	0.441 / 95	0.667 / 1
OFH	0.500 / 62	0.563 / 31	0.516 / 55	0.504 / 81	0.518 / 69	0.403 / 119	0.555 / 45	0.470 / 85	0.468 / 88
F-TV-L1	0.500 / 63	0.438 / 110	0.412 / 137	0.757 / 3	0.474 / 87	0.360 / 131	0.544 / 54	0.415 / 107	0.600 / 22
OFLAF	0.498 / 64	0.453 / 103	0.552 / 12	0.613 / 36	0.625 / 10	0.526 / 45	0.343 / 117	0.438 / 97	0.437 / 109
TriangleFlow	0.497 / 65	0.407 / 125	0.519 / 49	0.516 / 78	0.546 / 51	0.707 / 8	0.564 / 43	0.334 / 125	0.385 / 126
3DFlow	0.497 / 66	0.457 / 101	0.577 / 5	0.432 / 94	0.539 / 58	0.531 / 39	0.300 / 132	0.584 / 36	0.554 / 48
AggregFlow	0.496 / 67	0.411 / 121	0.535 / 28	0.572 / 53	0.442 / 102	0.529 / 40	0.674 / 20	0.367 / 119	0.439 / 107
S2F-IF	0.496 / 68	0.522 / 66	0.509 / 63	0.569 / 57	0.413 / 112	0.466 / 84	0.432 / 92	0.550 / 52	0.503 / 66
SRR-TV0F-NL	0.494 / 69	0.418 / 115	0.536 / 26	0.556 / 64	0.472 / 88	0.464 / 86	0.535 / 60	0.556 / 49	0.415 / 118
COFM	0.493 / 70	0.436 / 111	0.596 / 1	0.594 / 45	0.561 / 42	0.402 / 120	0.309 / 130	0.540 / 58	0.506 / 63
PMF	0.493 / 71	0.511 / 74	0.507 / 65	0.317 / 118	0.563 / 41	0.508 / 56	0.646 / 23	0.538 / 59	0.352 / 133
Layers++	0.493 / 72	0.516 / 70	0.504 / 70	0.651 / 27	0.547 / 49	0.443 / 101	0.236 / 139	0.615 / 28	0.431 / 113
FESL	0.492 / 73	0.483 / 88	0.510 / 61	0.576 / 50	0.541 / 56	0.430 / 111	0.498 / 71	0.498 / 76	0.398 / 123

TABLE V
SUBJECTIVE QUALITY VALUES AND THE RE-RANKING OF THE MIDDLEBURY BENCHMARK (PART II).

	Average value / rank	Mequon value / rank	Schefflera value / rank	Urban value / rank	Teddy value / rank	Backyard value / rank	Basketball value / rank	Dumptruck value / rank	Evergreen value / rank
Classic+NL	0.491 / 74	0.585 / 11	0.538 / 24	0.523 / 77	0.558 / 45	0.500 / 59	0.330 / 121	0.482 / 81	0.416 / 117
RFlow	0.491 / 75	0.466 / 96	0.542 / 20	0.611 / 37	0.449 / 100	0.472 / 80	0.390 / 105	0.439 / 96	0.555 / 47
Classic+CPF	0.490 / 76	0.528 / 56	0.536 / 27	0.467 / 90	0.592 / 19	0.477 / 76	0.412 / 101	0.543 / 57	0.365 / 132
SLK	0.489 / 77	0.417 / 117	0.427 / 133	0.388 / 101	0.470 / 92	0.640 / 18	0.626 / 30	0.385 / 117	0.563 / 37
FlowNetS+ft+v	0.489 / 78	0.524 / 63	0.432 / 130	0.555 / 65	0.573 / 34	0.392 / 123	0.607 / 34	0.276 / 135	0.555 / 45
H+S_ROB	0.488 / 79	0.545 / 44	0.439 / 128	0.307 / 121	0.399 / 118	0.702 / 9	0.455 / 86	0.472 / 84	0.582 / 29
FOLKI	0.487 / 80	0.453 / 104	0.490 / 92	0.414 / 97	0.533 / 61	0.311 / 136	0.570 / 42	0.517 / 67	0.610 / 15
DPOF	0.486 / 81	0.462 / 99	0.524 / 44	0.417 / 96	0.430 / 108	0.402 / 121	0.690 / 19	0.523 / 63	0.443 / 102
HBM-GC	0.486 / 82	0.556 / 35	0.476 / 103	0.665 / 21	0.575 / 31	0.468 / 81	0.245 / 136	0.388 / 115	0.512 / 62
Fusion	0.486 / 83	0.555 / 36	0.500 / 75	0.571 / 54	0.525 / 63	0.601 / 24	0.342 / 119	0.442 / 94	0.350 / 136
NL-TV-NCC	0.485 / 84	0.546 / 43	0.520 / 46	0.543 / 70	0.389 / 126	0.363 / 129	0.520 / 64	0.457 / 89	0.542 / 56
ROF-ND	0.485 / 85	0.418 / 116	0.485 / 97	0.619 / 34	0.452 / 99	0.500 / 60	0.389 / 106	0.580 / 38	0.437 / 108
Black & Anandan	0.482 / 86	0.523 / 65	0.511 / 60	0.155 / 140	0.591 / 20	0.504 / 57	0.414 / 100	0.553 / 51	0.606 / 18
Aniso-Texture	0.481 / 87	0.574 / 22	0.511 / 59	0.584 / 46	0.329 / 135	0.618 / 21	0.281 / 135	0.449 / 91	0.506 / 64
Sparse Occlusion	0.481 / 88	0.527 / 57	0.478 / 101	0.681 / 19	0.392 / 122	0.435 / 110	0.384 / 107	0.448 / 92	0.503 / 67
Adaptive	0.480 / 89	0.573 / 24	0.497 / 81	0.651 / 26	0.349 / 133	0.442 / 103	0.315 / 126	0.396 / 113	0.617 / 13
ACK-Prior	0.477 / 90	0.543 / 47	0.535 / 29	0.269 / 127	0.435 / 104	0.493 / 67	0.519 / 65	0.584 / 37	0.440 / 106
CPM-Flow	0.477 / 91	0.526 / 58	0.537 / 25	0.382 / 104	0.370 / 131	0.438 / 107	0.578 / 38	0.430 / 101	0.551 / 51
IAOF2	0.475 / 92	0.399 / 129	0.464 / 114	0.560 / 63	0.427 / 109	0.393 / 122	0.616 / 33	0.446 / 93	0.496 / 73
Horn & Schunck	0.474 / 93	0.503 / 77	0.424 / 135	0.264 / 128	0.514 / 71	0.514 / 50	0.538 / 57	0.501 / 75	0.531 / 58
Correlation Flow	0.473 / 94	0.525 / 61	0.557 / 11	0.527 / 74	0.397 / 119	0.627 / 20	0.329 / 122	0.353 / 121	0.468 / 89
ProbFlowFields	0.472 / 95	0.472 / 92	0.512 / 58	0.490 / 85	0.493 / 81	0.440 / 106	0.310 / 128	0.473 / 83	0.590 / 26
ComponentFusion	0.472 / 96	0.493 / 81	0.521 / 45	0.595 / 44	0.376 / 130	0.696 / 11	0.430 / 93	0.320 / 127	0.341 / 138
SVFilterOh	0.471 / 97	0.407 / 124	0.546 / 15	0.331 / 110	0.560 / 44	0.480 / 75	0.579 / 37	0.517 / 66	0.351 / 135
Steered-L1	0.471 / 98	0.541 / 48	0.503 / 73	0.294 / 124	0.245 / 141	0.493 / 66	0.554 / 47	0.504 / 73	0.632 / 8
Ramp	0.470 / 99	0.515 / 72	0.544 / 16	0.470 / 88	0.547 / 50	0.438 / 108	0.343 / 118	0.502 / 74	0.405 / 121
LSM	0.469 / 100	0.517 / 69	0.514 / 57	0.549 / 67	0.484 / 84	0.467 / 83	0.336 / 120	0.438 / 98	0.450 / 98
FlowNet2	0.469 / 101	0.387 / 132	0.475 / 105	0.525 / 75	0.510 / 72	0.442 / 102	0.634 / 26	0.337 / 124	0.443 / 103
CNN-flow-warp+ref	0.468 / 102	0.603 / 9	0.490 / 90	0.412 / 98	0.483 / 85	0.464 / 88	0.365 / 111	0.306 / 129	0.618 / 12
S2D-Matching	0.467 / 103	0.559 / 34	0.500 / 74	0.471 / 87	0.553 / 47	0.367 / 128	0.422 / 96	0.400 / 112	0.463 / 91
FlowFields	0.466 / 104	0.513 / 73	0.489 / 94	0.570 / 56	0.403 / 117	0.389 / 124	0.429 / 94	0.547 / 55	0.387 / 125
HCIC-L	0.464 / 105	0.410 / 122	0.421 / 136	0.435 / 93	0.393 / 121	0.646 / 17	0.575 / 39	0.387 / 116	0.448 / 100
StereoOF-V1MT	0.464 / 106	0.457 / 102	0.495 / 84	0.309 / 120	0.418 / 111	0.445 / 99	0.486 / 76	0.468 / 88	0.633 / 7
BriefMatch	0.458 / 107	0.518 / 68	0.499 / 78	0.223 / 135	0.506 / 75	0.482 / 69	0.309 / 129	0.649 / 17	0.480 / 79
EPMNet	0.458 / 108	0.402 / 128	0.473 / 107	0.569 / 58	0.393 / 120	0.409 / 117	0.552 / 48	0.411 / 109	0.452 / 96
Adaptive flow	0.458 / 109	0.377 / 134	0.499 / 79	0.505 / 80	0.522 / 65	0.481 / 72	0.326 / 123	0.571 / 44	0.381 / 128
StereoFlow	0.457 / 110	0.369 / 136	0.464 / 115	0.597 / 42	0.351 / 132	0.503 / 58	0.441 / 91	0.438 / 99	0.497 / 72
2D-CLG	0.454 / 111	0.564 / 28	0.446 / 126	0.324 / 113	0.454 / 98	0.420 / 115	0.361 / 112	0.413 / 108	0.646 / 3
Nguyen	0.453 / 112	0.464 / 97	0.396 / 139	0.640 / 32	0.490 / 82	0.354 / 132	0.482 / 78	0.305 / 130	0.494 / 75
HAST	0.453 / 113	0.548 / 42	0.531 / 37	0.398 / 100	0.584 / 26	0.345 / 133	0.409 / 102	0.402 / 111	0.406 / 120
EPPM w/o HM	0.452 / 114	0.439 / 109	0.473 / 108	0.316 / 119	0.379 / 129	0.526 / 44	0.662 / 22	0.428 / 102	0.394 / 124
CostFilter	0.452 / 115	0.488 / 85	0.543 / 18	0.383 / 103	0.471 / 91	0.441 / 104	0.521 / 63	0.422 / 105	0.347 / 137
UnFlow	0.451 / 116	0.458 / 100	0.449 / 125	0.564 / 59	0.497 / 78	0.423 / 114	0.238 / 138	0.505 / 72	0.475 / 86
Complementary OF	0.450 / 117	0.520 / 67	0.524 / 43	0.321 / 114	0.466 / 95	0.373 / 126	0.454 / 87	0.468 / 87	0.475 / 84
IAOF	0.445 / 118	0.405 / 126	0.454 / 119	0.277 / 125	0.434 / 105	0.460 / 90	0.523 / 62	0.469 / 86	0.540 / 57
FC-2Layers-FF	0.445 / 119	0.379 / 133	0.519 / 48	0.570 / 55	0.520 / 66	0.448 / 96	0.299 / 133	0.405 / 110	0.418 / 116
TVL1_ROB	0.441 / 120	0.495 / 79	0.497 / 83	0.540 / 72	0.470 / 93	0.320 / 134	0.369 / 110	0.276 / 134	0.561 / 42
TV-L1-improved	0.438 / 121	0.544 / 46	0.454 / 120	0.215 / 137	0.442 / 101	0.526 / 43	0.418 / 98	0.362 / 120	0.546 / 53
Pyramid LK	0.435 / 122	0.476 / 89	0.478 / 102	0.210 / 139	0.433 / 107	0.596 / 25	0.483 / 77	0.347 / 122	0.454 / 93
SegOF	0.434 / 123	0.411 / 119	0.428 / 132	0.357 / 107	0.323 / 137	0.555 / 32	0.498 / 72	0.417 / 106	0.479 / 80
EpicFlow	0.433 / 124	0.491 / 83	0.474 / 106	0.379 / 105	0.391 / 123	0.496 / 64	0.538 / 58	0.344 / 123	0.352 / 134
Shiralkar	0.432 / 125	0.499 / 78	0.469 / 110	0.325 / 111	0.382 / 128	0.406 / 118	0.513 / 69	0.297 / 132	0.563 / 38
Efficient-NL	0.428 / 126	0.490 / 84	0.461 / 116	0.298 / 123	0.567 / 36	0.429 / 112	0.480 / 79	0.314 / 128	0.382 / 127
HBpMotionGpu	0.426 / 127	0.370 / 135	0.429 / 131	0.536 / 73	0.407 / 115	0.385 / 125	0.170 / 140	0.615 / 27	0.500 / 70
GraphCuts	0.426 / 128	0.342 / 139	0.469 / 111	0.238 / 130	0.507 / 74	0.542 / 36	0.356 / 113	0.493 / 79	0.463 / 90
Dynamic MRF	0.421 / 129	0.504 / 76	0.500 / 76	0.236 / 131	0.518 / 70	0.461 / 89	0.320 / 125	0.278 / 133	0.548 / 52
PGM-C	0.420 / 130	0.473 / 90	0.504 / 69	0.300 / 122	0.329 / 136	0.445 / 100	0.544 / 53	0.435 / 100	0.333 / 139
2bit-BM-tele	0.412 / 131	0.411 / 120	0.538 / 23	0.340 / 109	0.628 / 9	0.285 / 140	0.344 / 116	0.194 / 141	0.555 / 46
SimpleFlow	0.408 / 132	0.575 / 20	0.508 / 64	0.224 / 134	0.321 / 138	0.441 / 105	0.416 / 99	0.304 / 131	0.479 / 81
IIOF-NLDP	0.407 / 133	0.403 / 127	0.520 / 47	0.406 / 99	0.437 / 103	0.499 / 61	0.303 / 131	0.200 / 140	0.489 / 77
LocallyOriented	0.406 / 134	0.452 / 106	0.450 / 123	0.319 / 117	0.344 / 134	0.451 / 95	0.350 / 115	0.377 / 118	0.502 / 69
Rannacher	0.388 / 135	0.473 / 91	0.482 / 99	0.233 / 133	0.302 / 139	0.560 / 30	0.241 / 137	0.389 / 114	0.421 / 115
FFV1MT	0.385 / 136	0.351 / 138	0.389 / 141	0.260 / 129	0.388 / 127	0.474 / 79	0.488 / 74	0.236 / 137	0.497 / 71
AdaConv-v1	0.381 / 137	0.358 / 137	0.449 / 124	0.215 / 138	0.493 / 80	0.246 / 141	0.465 / 84	0.450 / 90	0.368 / 130
Heeger++	0.372 / 138	0.336 / 140	0.389 / 140	0.319 / 116	0.405 / 116	0.464 / 87	0.399 / 103	0.229 / 138	0.435 / 110
GroupFlow	0.359 / 139	0.399 / 130	0.434 / 129	0.130 / 141	0.287 / 140	0.447 / 98	0.448 / 89	0.324 / 126	0.403 / 122
SPSA-learn	0.346 / 140	0.398 / 131	0.500 / 77	0.215 / 136	0.465 / 96	0.296 / 137	0.282 / 134	0.243 / 136	0.368 / 129
Periodicity	0.295 / 141	0.297 / 141	0.406 / 138	0.233 / 132	0.434 / 106	0.369 / 127	0.168 / 141	0.215 / 139	0.240 / 141

TABLE VI

RE-RANKING OF THE MIDDLEBURY BENCHMARK. NEW: RE-RANKING GIVEN BY SUBJECTIVE STUDY. OLD: RANKING IN THE MIDDLEBURY BENCHMARK (PART I).

	Average new / old	Mequon new / old	Schefflera new / old	Urban new / old	Teddy new / old	Backyard new / old	Basketball new / old	Dumptruck new / old	Evergreen new / old
SuperSlomo	1 / 5	3 / 2	71 / 34	1 / 1	2 / 2	6 / 1	8 / 3	1 / 1	32 / 3
CtxSyn	2 / 1	2 / 1	3 / 1	91 / 63	1 / 1	1 / 2	13 / 1	2 / 3	61 / 2
DeepFlow2	3 / 9	26 / 24	39 / 57	9 / 8	23 / 21	26 / 39	3 / 6	18 / 22	9 / 31
SuperFlow	4 / 10	13 / 15	104 / 70	82 / 41	46 / 40	5 / 9	4 / 25	10 / 31	5 / 7
DeepFlow	5 / 7	51 / 22	13 / 56	16 / 7	17 / 26	38 / 40	11 / 10	8 / 4	21 / 30
ALD-Flow	6 / 21	27 / 95	2 / 48	22 / 6	15 / 49	116 / 26	1 / 12	12 / 7	82 / 74
PMMST	7 / 4	7 / 10	31 / 15	17 / 4	77 / 20	19 / 6	5 / 5	32 / 9	68 / 9
Aniso. Huber-L1	8 / 13	18 / 16	32 / 99	35 / 24	12 / 10	47 / 46	24 / 11	11 / 23	10 / 15
SIOF	9 / 28	49 / 38	36 / 98	24 / 52	25 / 28	12 / 4	21 / 21	45 / 16	35 / 48
CBF	10 / 8	17 / 4	40 / 66	12 / 9	14 / 5	27 / 3	40 / 13	29 / 39	30 / 12
Bartels	11 / 77	86 / 115	22 / 72	18 / 22	64 / 77	7 / 12	73 / 102	3 / 17	33 / 58
IROF++	12 / 17	4 / 31	6 / 26	71 / 64	7 / 3	77 / 36	6 / 45	19 / 18	83 / 55
LDOF	13 / 41	25 / 32	98 / 74	89 / 65	4 / 35	2 / 8	17 / 50	80 / 79	41 / 11
RNLOD-Flow	14 / 71	80 / 37	4 / 63	33 / 72	33 / 15	10 / 105	52 / 92	24 / 47	44 / 100
2nd-order prior	15 / 24	14 / 11	72 / 87	38 / 28	60 / 27	23 / 48	70 / 27	5 / 24	16 / 40
SepConv-v1	16 / 6	6 / 3	95 / 23	83 / 50	8 / 30	68 / 7	15 / 4	41 / 2	2 / 1
DF-Auto	17 / 20	95 / 14	7 / 69	41 / 30	55 / 22	3 / 15	28 / 31	78 / 52	31 / 18
MDP-Flow2	18 / 3	19 / 8	89 / 10	20 / 13	13 / 4	28 / 5	49 / 24	13 / 8	95 / 24
CLG-TV	19 / 15	41 / 13	96 / 88	47 / 17	6 / 16	74 / 47	46 / 9	9 / 20	11 / 25
FGIK	20 / 2	15 / 5	113 / 112	112 / 113	16 / 124	15 / 100	12 / 81	7 / 131	59 / 117
IROF-TV	21 / 14	53 / 40	50 / 40	15 / 20	11 / 7	54 / 37	32 / 49	61 / 44	49 / 16
LME	22 / 16	23 / 17	54 / 37	40 / 40	24 / 23	49 / 59	36 / 40	15 / 6	76 / 32
TC/T-Flow	23 / 38	59 / 83	19 / 61	4 / 18	79 / 79	94 / 53	2 / 33	103 / 92	43 / 60
Modified CLG	24 / 35	12 / 7	134 / 106	25 / 49	21 / 46	14 / 25	104 / 48	25 / 14	20 / 35
CombBMOF	25 / 19	87 / 69	9 / 20	61 / 37	18 / 58	65 / 22	16 / 32	50 / 42	54 / 26
CRTflow	26 / 48	40 / 47	34 / 95	79 / 48	68 / 14	82 / 38	18 / 20	20 / 89	25 / 64
p-harmonic	27 / 25	10 / 26	51 / 92	31 / 5	32 / 59	53 / 41	80 / 16	22 / 29	55 / 44
TV-L1-MCT	28 / 46	112 / 77	38 / 53	76 / 75	57 / 19	63 / 118	27 / 19	6 / 62	19 / 19
OAR-Flow	29 / 31	64 / 61	112 / 51	2 / 12	5 / 54	91 / 64	68 / 23	64 / 55	50 / 57
FMOF	30 / 27	8 / 71	30 / 13	108 / 80	29 / 62	35 / 16	9 / 60	42 / 26	60 / 54
NNF-Local	31 / 12	30 / 12	42 / 3	30 / 11	28 / 67	37 / 11	50 / 53	40 / 19	92 / 13
Brox et al.	32 / 26	71 / 42	14 / 50	51 / 32	22 / 11	41 / 18	75 / 80	56 / 93	4 / 6
DMF_ROB	33 / 40	45 / 66	66 / 64	11 / 105	67 / 64	73 / 42	81 / 18	39 / 27	34 / 56
TI-DOFE	34 / 103	114 / 110	91 / 137	48 / 53	62 / 123	42 / 31	25 / 78	33 / 65	14 / 106
WLIF-Flow	35 / 22	1 / 18	33 / 35	66 / 59	30 / 9	93 / 21	41 / 99	26 / 11	131 / 38
Ad-TV-NDC	36 / 34	118 / 85	56 / 127	5 / 16	39 / 86	138 / 29	66 / 36	4 / 33	36 / 8
MLDP_OF	37 / 57	50 / 45	85 / 71	13 / 14	73 / 68	31 / 80	59 / 91	47 / 36	111 / 62
TCOF	38 / 70	93 / 59	68 / 119	52 / 46	35 / 31	29 / 77	35 / 54	71 / 118	78 / 93
Local-TV-L1	39 / 30	54 / 25	87 / 101	8 / 2	3 / 25	135 / 60	88 / 30	77 / 30	17 / 10
Classic++	40 / 53	29 / 35	86 / 75	10 / 23	76 / 63	71 / 91	83 / 88	82 / 78	28 / 68
nLayers	41 / 44	37 / 33	41 / 11	39 / 108	43 / 57	22 / 120	90 / 87	65 / 21	119 / 45
2DHMM-SAS	42 / 37	21 / 49	93 / 77	106 / 69	38 / 24	55 / 76	14 / 43	53 / 54	94 / 63
Filter Flow	43 / 66	75 / 60	121 / 115	62 / 58	114 / 81	16 / 17	44 / 55	60 / 67	65 / 46
MDP-Flow	44 / 29	5 / 6	52 / 14	43 / 36	94 / 50	46 / 63	109 / 93	31 / 34	87 / 33
JOF	45 / 32	52 / 44	17 / 12	29 / 29	37 / 32	78 / 78	124 / 94	16 / 15	112 / 50
PH-Flow	46 / 23	107 / 58	35 / 6	14 / 19	48 / 6	48 / 14	108 / 109	23 / 46	114 / 39
TC-Flow	47 / 49	108 / 101	109 / 62	6 / 10	59 / 60	97 / 65	67 / 46	43 / 43	104 / 96
NN-field	48 / 11	32 / 23	67 / 4	95 / 85	89 / 90	34 / 13	51 / 35	30 / 10	74 / 20
Learning Flow	49 / 124	39 / 63	62 / 108	84 / 141	54 / 107	52 / 130	56 / 79	104 / 74	24 / 114
PGAM+LK	50 / 135	98 / 132	100 / 126	126 / 132	113 / 136	4 / 103	29 / 106	46 / 72	39 / 107
AGIF+OF	51 / 51	55 / 55	8 / 31	49 / 34	27 / 36	51 / 87	97 / 114	21 / 48	140 / 101
ORFR	52 / 125	123 / 130	82 / 111	86 / 81	83 / 94	33 / 132	10 / 126	69 / 113	99 / 122
BlockOverlap	53 / 56	62 / 21	21 / 96	69 / 60	53 / 47	70 / 51	114 / 51	70 / 37	6 / 5
NNF-EAC	54 / 18	33 / 29	117 / 29	92 / 51	97 / 39	130 / 62	7 / 8	48 / 13	85 / 29
TriFlow	55 / 89	105 / 127	80 / 91	23 / 39	125 / 104	92 / 84	55 / 101	68 / 61	27 / 73
ComplOF-FED-GPU	56 / 45	16 / 86	88 / 44	102 / 103	40 / 41	113 / 50	82 / 22	34 / 66	40 / 81
FlowFields+	57 / 65	60 / 62	118 / 19	60 / 89	90 / 92	85 / 54	61 / 74	35 / 51	105 / 69
Sparse-NonSparse	58 / 54	38 / 41	53 / 27	28 / 62	86 / 18	109 / 107	95 / 86	62 / 98	101 / 78
SILK	59 / 122	113 / 113	122 / 135	115 / 137	52 / 115	13 / 99	127 / 110	14 / 40	23 / 66
Occlusion-TV-L1	60 / 78	82 / 64	127 / 105	7 / 3	124 / 108	62 / 44	85 / 58	54 / 80	97 / 87
TF+OM	61 / 64	94 / 104	10 / 33	68 / 27	110 / 91	139 / 68	31 / 57	95 / 77	1 / 53
OFF	62 / 90	31 / 79	55 / 78	81 / 84	69 / 73	119 / 81	45 / 41	85 / 90	88 / 108
F-TV-L1	63 / 33	110 / 98	137 / 97	3 / 25	87 / 56	131 / 32	54 / 7	107 / 32	22 / 14
OFLAF	64 / 61	103 / 51	12 / 8	36 / 21	10 / 13	45 / 117	117 / 77	97 / 121	109 / 102
TriangleFlow	65 / 110	125 / 89	49 / 90	78 / 82	51 / 69	8 / 93	43 / 85	125 / 128	126 / 137
3DFlow	66 / 91	101 / 91	5 / 39	94 / 77	58 / 72	39 / 66	132 / 125	36 / 91	48 / 77
AggregFlow	67 / 74	121 / 128	28 / 55	53 / 55	102 / 97	40 / 19	20 / 26	119 / 99	107 / 79
S2F-IF	68 / 58	66 / 93	63 / 18	57 / 45	112 / 80	84 / 95	92 / 52	52 / 45	66 / 88
SRR-TVOF-NL	69 / 87	115 / 102	26 / 65	64 / 83	88 / 89	86 / 67	60 / 104	49 / 49	118 / 92
COFM	70 / 39	111 / 30	1 / 22	45 / 26	42 / 29	120 / 24	130 / 123	58 / 60	63 / 41
PMF	71 / 59	74 / 65	65 / 43	118 / 104	41 / 65	56 / 27	23 / 67	59 / 84	133 / 110
Layers++	72 / 43	70 / 19	70 / 2	27 / 42	49 / 37	101 / 135	139 / 128	28 / 25	113 / 34
FESL	73 / 86	88 / 70	61 / 32	50 / 70	56 / 61	111 / 121	71 / 98	76 / 101	123 / 97

TABLE VII

RE-RANKING OF THE MIDDLEBURY BENCHMARK. NEW: RE-RANKING GIVEN BY SUBJECTIVE STUDY. OLD: RANKING IN THE MIDDLEBURY BENCHMARK (PART II).

	Average new / old	Mequon new / old	Schefflera new / old	Urban new / old	Teddy new / old	Backyard new / old	Basketball new / old	Dumptruck new / old	Evergreen new / old
Classic+NL	74 / 75	11 / 50	24 / 36	77 / 91	45 / 17	59 / 106	121 / 96	81 / 105	117 / 83
RFlow	75 / 88	96 / 46	20 / 93	37 / 92	100 / 78	80 / 52	105 / 66	96 / 88	47 / 76
Classic+CPF	76 / 81	56 / 56	27 / 42	90 / 71	19 / 12	76 / 127	101 / 127	57 / 106	132 / 119
SLK	77 / 137	117 / 117	133 / 125	101 / 135	92 / 135	18 / 133	30 / 83	117 / 133	37 / 129
FlowNetS+ft+v	78 / 62	63 / 39	130 / 116	65 / 38	34 / 44	123 / 79	34 / 15	135 / 95	45 / 21
H+S_ROB	79 / 127	44 / 111	128 / 114	121 / 138	118 / 125	9 / 101	86 / 82	84 / 132	29 / 126
FOLKI	80 / 119	104 / 125	92 / 138	97 / 102	61 / 134	136 / 74	42 / 71	67 / 59	15 / 49
DPOF	81 / 50	99 / 105	44 / 7	96 / 96	108 / 76	121 / 43	19 / 70	63 / 57	102 / 72
HBM-GC	82 / 80	35 / 43	103 / 67	21 / 31	31 / 43	81 / 128	136 / 136	115 / 82	62 / 36
Fusion	83 / 73	36 / 34	75 / 45	54 / 43	63 / 70	24 / 94	119 / 120	94 / 83	136 / 105
NL-TV-NCC	84 / 107	43 / 108	46 / 86	70 / 73	126 / 130	129 / 23	64 / 115	89 / 116	56 / 99
ROF-ND	85 / 113	116 / 80	97 / 81	34 / 57	99 / 126	60 / 102	106 / 116	38 / 70	108 / 132
Black & Anandan	86 / 69	65 / 84	60 / 129	140 / 126	20 / 106	57 / 33	100 / 42	51 / 71	18 / 17
Aniso-Texture	87 / 117	22 / 53	59 / 107	46 / 90	135 / 132	21 / 126	135 / 132	91 / 76	64 / 115
Sparse Occlusion	88 / 60	57 / 73	101 / 82	19 / 15	122 / 55	110 / 111	107 / 38	92 / 87	67 / 80
Adaptive	89 / 98	24 / 88	81 / 117	26 / 33	133 / 75	103 / 122	126 / 69	113 / 115	13 / 59
ACK-Prior	90 / 114	47 / 97	29 / 49	127 / 125	104 / 95	67 / 129	65 / 117	37 / 81	106 / 109
CPM-Flow	91 / 36	58 / 74	25 / 21	104 / 56	131 / 98	107 / 55	38 / 39	101 / 28	51 / 61
IAOF2	92 / 109	129 / 112	114 / 121	63 / 74	109 / 87	122 / 124	33 / 112	93 / 73	73 / 71
Horn & Schunck	93 / 85	77 / 72	135 / 130	128 / 118	71 / 119	50 / 34	57 / 29	75 / 96	58 / 42
Correlation Flow	94 / 112	61 / 94	11 / 100	74 / 35	119 / 83	20 / 123	122 / 135	121 / 134	89 / 120
ProbFlowFields	95 / 55	92 / 68	58 / 16	85 / 99	81 / 33	106 / 49	128 / 59	83 / 56	26 / 28
ComponentFusion	96 / 76	81 / 109	45 / 30	44 / 54	130 / 52	11 / 90	93 / 37	127 / 120	138 / 116
SVFilterOh	97 / 95	124 / 87	15 / 17	110 / 116	44 / 66	75 / 92	37 / 119	66 / 53	135 / 86
Steered-L1	98 / 97	48 / 20	73 / 47	124 / 129	141 / 113	66 / 98	47 / 64	73 / 69	8 / 89
Ramp	99 / 72	72 / 54	16 / 28	88 / 93	50 / 8	108 / 104	118 / 113	74 / 104	121 / 82
LSM	100 / 68	69 / 57	57 / 38	67 / 68	84 / 45	83 / 108	120 / 107	98 / 102	98 / 90
FlowNet2	101 / 96	132 / 136	105 / 80	75 / 88	72 / 110	102 / 70	26 / 56	124 / 85	103 / 52
CNN-flow-warp+ref	102 / 79	9 / 9	90 / 76	98 / 94	85 / 99	88 / 83	111 / 17	129 / 112	12 / 43
S2D-Matching	103 / 93	34 / 82	74 / 68	87 / 79	47 / 38	128 / 88	96 / 118	112 / 63	91 / 67
FlowFields	104 / 42	73 / 67	94 / 24	56 / 86	117 / 74	124 / 28	94 / 73	55 / 35	125 / 65
HCIC-L	105 / 138	122 / 139	136 / 132	93 / 111	121 / 133	17 / 35	39 / 139	116 / 117	100 / 136
StereoOF-V1MT	106 / 115	102 / 120	84 / 89	120 / 117	111 / 129	99 / 73	76 / 84	88 / 125	7 / 51
BriefMatch	107 / 106	68 / 90	78 / 54	135 / 119	75 / 121	69 / 45	129 / 100	17 / 58	79 / 70
EPMNet	108 / 108	128 / 137	107 / 73	58 / 87	120 / 138	117 / 75	48 / 90	109 / 86	96 / 94
Adaptive flow	109 / 126	134 / 123	79 / 136	80 / 78	65 / 116	72 / 137	123 / 133	44 / 38	128 / 104
StereoFlow	110 / 129	136 / 141	115 / 134	42 / 47	132 / 71	58 / 139	91 / 140	99 / 50	72 / 125
2D-CLG	111 / 83	28 / 27	126 / 118	113 / 101	98 / 93	115 / 97	112 / 14	108 / 110	3 / 23
Nguyen	112 / 92	97 / 92	139 / 131	32 / 44	82 / 103	132 / 57	78 / 68	130 / 123	75 / 37
HAST	113 / 63	42 / 28	37 / 9	100 / 122	26 / 34	133 / 61	102 / 131	111 / 97	120 / 91
EPPM w/o HM	114 / 104	109 / 106	108 / 52	119 / 124	129 / 102	44 / 20	22 / 121	102 / 108	124 / 98
CostFilter	115 / 94	85 / 114	18 / 41	103 / 110	91 / 112	104 / 72	63 / 47	105 / 109	137 / 123
UnFlow	116 / 128	100 / 131	125 / 103	59 / 95	78 / 85	114 / 136	138 / 134	72 / 41	86 / 138
Complementary OF	117 / 101	67 / 116	43 / 58	114 / 133	95 / 109	126 / 85	87 / 44	87 / 94	84 / 131
IAOF	118 / 100	126 / 119	119 / 139	125 / 112	105 / 101	90 / 56	62 / 61	86 / 75	57 / 47
FC-2Layers-FF	119 / 84	133 / 78	48 / 5	55 / 67	66 / 48	96 / 109	133 / 122	110 / 111	116 / 85
TVL1_ROB	120 / 99	79 / 103	83 / 133	72 / 76	93 / 105	134 / 30	110 / 63	134 / 114	42 / 22
TV-L1-improved	121 / 102	46 / 48	120 / 113	137 / 114	101 / 42	43 / 89	98 / 95	120 / 124	53 / 75
Pyramid LK	122 / 139	89 / 134	102 / 140	139 / 139	107 / 141	25 / 140	77 / 89	122 / 136	93 / 141
SegOF	123 / 134	119 / 118	132 / 83	107 / 131	137 / 137	32 / 131	72 / 105	106 / 135	80 / 124
EpicFlow	124 / 67	83 / 75	106 / 46	105 / 61	123 / 111	64 / 71	58 / 34	123 / 64	134 / 121
Shiralkar	125 / 120	78 / 122	110 / 104	111 / 107	128 / 131	118 / 116	69 / 76	132 / 126	38 / 134
Efficient-NL	126 / 82	84 / 36	116 / 60	123 / 115	36 / 53	112 / 110	79 / 111	128 / 107	127 / 111
HBpMotionGpu	127 / 116	135 / 124	131 / 128	73 / 66	115 / 114	125 / 113	140 / 108	27 / 12	70 / 84
GraphCuts	128 / 105	139 / 126	111 / 59	130 / 127	74 / 88	36 / 96	113 / 72	79 / 100	90 / 113
Dynamic MRF	129 / 118	76 / 81	76 / 79	131 / 106	70 / 118	89 / 58	125 / 124	133 / 119	52 / 112
PGM-C	130 / 52	90 / 76	69 / 25	122 / 98	136 / 100	100 / 69	53 / 28	100 / 68	139 / 103
2bit-BM-tele	131 / 130	120 / 99	23 / 110	109 / 120	9 / 84	140 / 82	116 / 137	141 / 141	46 / 27
SimpleFlow	132 / 121	20 / 52	64 / 84	134 / 136	138 / 51	105 / 119	99 / 129	131 / 137	81 / 133
IIOF-NLDP	133 / 131	127 / 107	47 / 85	99 / 100	103 / 96	61 / 125	131 / 130	140 / 140	77 / 128
LocallyOriented	134 / 111	106 / 96	123 / 122	117 / 109	134 / 117	95 / 114	115 / 75	118 / 103	69 / 95
Rannacher	135 / 123	91 / 100	99 / 120	133 / 121	139 / 82	30 / 112	137 / 97	114 / 122	115 / 118
FFV1MT	136 / 133	138 / 133	141 / 124	129 / 123	127 / 127	79 / 86	74 / 103	137 / 127	71 / 127
AdaConv-v1	137 / 47	137 / 121	124 / 94	138 / 97	80 / 122	141 / 10	84 / 2	90 / 5	130 / 4
Heeger++	138 / 136	140 / 135	140 / 123	116 / 128	116 / 128	87 / 134	103 / 65	138 / 129	110 / 130
GroupFlow	139 / 140	130 / 138	129 / 109	141 / 130	140 / 139	98 / 138	89 / 138	126 / 130	122 / 135
SPSA-learn	140 / 132	131 / 129	77 / 102	136 / 134	96 / 120	137 / 115	134 / 62	136 / 138	129 / 140
Periodicity	141 / 141	141 / 140	138 / 141	132 / 140	106 / 140	127 / 141	141 / 141	139 / 139	141 / 139